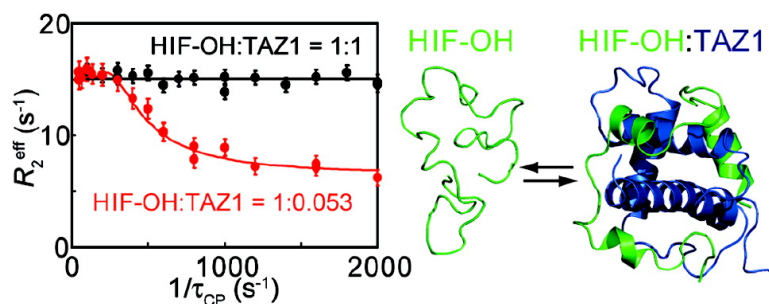


Tailoring Relaxation Dispersion Experiments for Fast-Associating Protein Complexes

Kenji Sugase, Jonathan C. Lansing, H. Jane Dyson, and Peter E. Wright

J. Am. Chem. Soc., **2007**, 129 (44), 13406-13407 • DOI: 10.1021/ja0762238 • Publication Date (Web): 13 October 2007

Downloaded from <http://pubs.acs.org> on February 14, 2009



More About This Article

Additional resources and features associated with this article are available within the HTML version:

- Supporting Information
- Access to high resolution figures
- Links to articles and content related to this article
- Copyright permission to reproduce figures and/or text from this article

[View the Full Text HTML](#)

Tailoring Relaxation Dispersion Experiments for Fast-Associating Protein Complexes

Kenji Sugase,[†] Jonathan C. Lansing,[‡] H. Jane Dyson, and Peter E. Wright*

Department of Molecular Biology and Skaggs Institute of Chemical Biology, The Scripps Research Institute, 10550 North Torrey Pines Road, La Jolla, California 92037

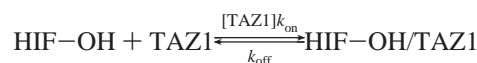
Received August 24, 2007; E-mail: wright@scripps.edu

NMR relaxation dispersion spectroscopy^{1–3} is a very powerful technique to characterize chemical and conformational exchange processes in proteins and other biologically important molecules on μs – ms timescales.⁴ Many of these processes proceed through weakly populated higher energy states that are difficult to detect experimentally. A major advantage of the relaxation dispersion method is that it can provide information on the structure of invisible high energy intermediates by analyzing the relaxation rates of an observable state that interconverts with them.⁵

We recently developed a method combining ¹⁵N R_2 relaxation dispersion spectroscopy and NMR titration to elucidate the mechanism of protein–protein binding reactions and in particular the coupled folding and binding processes that occur when an intrinsically disordered protein binds to its target.⁶ The method was applied to study binding of the phosphorylated kinase inducible domain (pKID) of the transcription factor CREB to the KIX domain of the CREB binding protein (CBP). By measuring ¹⁵N R_2 dispersions of pKID in the bound form as a function of pKID/KIX concentration ratio, we showed that pKID forms weak nonspecific encounter complexes with KIX that evolve via a folding intermediate to the fully bound state. Although our method is potentially applicable to a broad spectrum of biological interactions, it can be difficult to optimize the concentration ratios that give relaxation dispersions of sufficient amplitude to determine accurate kinetic and thermodynamic parameters. In this Communication, we describe methods for measuring relaxation dispersion in cases of very tight binding or loss of resonances in the bound state owing to intermediate exchange.

As an example, we consider binding of the Asn803-hydroxylated hypoxia-inducible factor-1 α (HIF–OH) to the transcriptional adapter zinc finger (TAZ1) domain of CBP.^{7–9} Although HIF–OH binds to TAZ1 by a coupled folding and binding mechanism (Supporting Information (SI) Figure S1) similar to the binding of pKID to KIX,⁶ we observe no ¹⁵N R_2 dispersion for HIF–OH in the fully bound state, that is, at concentration ratios close to 1:1 that were appropriate for study of the lower-affinity pKID/KIX complex (SI Figure S2).

We therefore analyzed ¹⁵N R_2 dispersions of the *free* HIF–OH resonances in samples containing substoichiometric amounts of TAZ1; no dispersion was observed in the absence of TAZ1. In contrast to experiments performed on the bound state of HIF–OH in the presence of equimolar TAZ1, high quality R_2 dispersion curves were obtained (Figure 1) and could be fitted well to a two-site exchange model:



where the fitting parameters are the chemical shift difference between the free and bound states, $\Delta\omega_{\text{FB}}$, the population-average intrinsic relaxation rate, R_2^0 , the association and dissociation rate constants, k_{on} and k_{off} , and the total concentrations of HIF–OH and TAZ1 (denoted $[\text{HIF-OH}]_0$ and $[\text{TAZ1}]_0$, respectively). The free TAZ1 concentration, $[\text{TAZ1}]$, is calculated from K_{D} , $[\text{HIF-OH}]_0$, and $[\text{TAZ1}]_0$.

For simplicity, we focused on the C-terminal α -helix (residues 816–825), which forms a distinctive binding element in the HIF–1 α /TAZ1 complex^{7,8} and fitted the dispersion curves to a global exchange process with fixed k_{on} and k_{off} values for all residues. The chemical shift changes $\Delta\omega_{\text{FB}}$ determined from the R_2 dispersion data correlate well with equilibrium chemical shift changes measured from NMR titration of HIF–OH with TAZ1 (SI Figure S4). The linear correlation with slope near 1 indicates that the weakly populated state detected by the R_2 dispersion experiment is the TAZ1-bound form.

Since the k_{on} obtained from these measurements (Table 1) is on the same order as translational diffusion,¹⁰ we infer that HIF–OH binding to TAZ1 is diffusion limited.

The k_{on} value is greater by 3 orders of magnitude than that for pKID/KIX complex formation ($10^6 \text{ M}^{-1}\cdot\text{s}^{-1}$).⁶ The difference suggests that we were not able to observe R_2 dispersions in the bound state for the HIF–OH/TAZ1 complex because k_{on} is very fast. To understand how the relative concentrations of the binding partners affect the R_2 dispersion profile, we simulated¹¹ the dependence of the effective R_2 relaxation rate, $R_2^{\text{eff}} (= R_2^0 + R_{\text{ex}})$, on the concentration ratio, $[\text{TAZ1}]_0/[\text{HIF-OH}]_0$, using the parameters obtained from the relaxation dispersion analysis (Figure 2a). R_{ex} is the excess contribution to R_2^{eff} caused by the exchange process.

Our previous experience of R_2 dispersion curve fitting suggests that R_{ex} should be moderate, ~ 3 to 25 s^{-1} , as shown by the gray area (concentration ratio of ~ 0.02 to 0.12 for the HIF–OH/TAZ1 system), in order to obtain reliable kinetic and thermodynamic parameters from the fits. The concentration ratios that gave good R_2 dispersion curves in the experiment (0.021 – 0.053) indeed fall into this range. When R_{ex} is too large, the NMR peak will be very broad (or unobservable), resulting in an R_2 dispersion curve with low signal/noise. On the other hand, R_{ex} is completely suppressed in the presence of excess TAZ1, because the HIF–OH/TAZ1 complex is of sufficiently high affinity (ca. 70 nM by ITC) that the population in the free state is very low. In this case, R_2^{eff} reaches the limiting value of R_2^0 for the bound state and there will be no R_2 dispersion. R_{ex} is determined by the ratio of the exchange rate, which is a sum of the forward and backward rates ($[\text{TAZ1}]k_{\text{on}} + k_{\text{off}}$), to the chemical shift difference. Since the forward rate, $[\text{TAZ1}]k_{\text{on}}$, is the only parameter that depends on the concentration ratio,

[†] Current address: Suntory Institute for Bioorganic Research, 1-1-1 Wakayama-dai, Shimamoto-cho, Mishima-gun, Osaka 618-8503, Japan.

[‡] Current address: Momenta Pharmaceuticals, 675 West Kendall Street, Cambridge MA 02142.

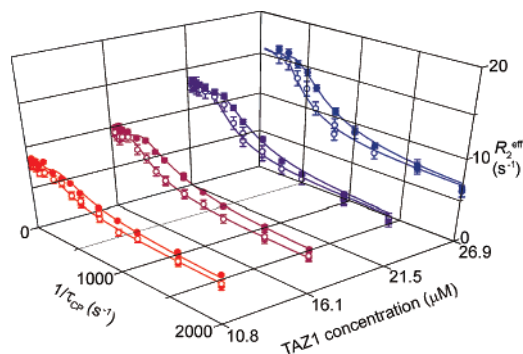


Figure 1. ^{15}N R_2 dispersion profiles for Arg820 of HIF–OH recorded for $510\ \mu\text{M}$ $[^{15}\text{N}]$ -HIF–OH in the presence of substoichiometric amounts of TAZ1. Data were acquired at 900 MHz (filled circles) and 600 MHz (open circles) using relaxation compensated Carr–Purcell–Meiboom–Gill (CPMG) pulse sequences.^{1,12} Curves for all observable dispersions are shown in Supporting Information Figure S3.

Table 1. R_2 Dispersion with Two-Site Exchange

parameter	value (fitting)
[HIF–OH] ₀ [μM]	505 (62) ^a
[TAZ1] ₀ [μM]	26.9 (3.2) ^{a,b}
$k_{\text{on}} \times 10^9$ [$\text{M}^{-1}\cdot\text{s}^{-1}$]	1.29 (0.94) ^a
k_{off} [s^{-1}]	185 (7.6) ^a
K_{D} [nM]	143 ^c

^a Values in parentheses are standard deviations. ^b Determined for the sample with the largest amount of TAZ1. The concentrations of TAZ1 in other samples were scaled by 0.4, 0.6, and 0.8. ^c Calculated according to the formula: $K_{\text{D}} = k_{\text{off}}/k_{\text{on}}$. This value is in reasonable agreement with the K_{D} of 70 nM measured by isothermal titration calorimetry (unpublished data). Fits to three-site exchange models failed to reproduce the measured K_{D} .

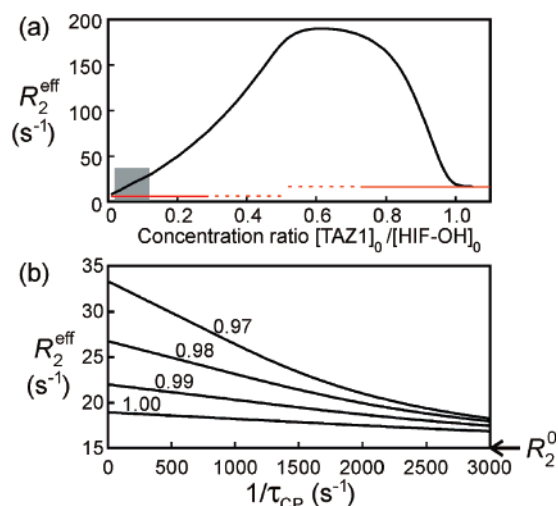


Figure 2. R_2^{eff} rates for Arg820 of HIF–OH simulated using the parameters listed in Table 1. (a) R_2^{eff} rates versus the concentration ratio, $[\text{TAZ1}]_0/[\text{HIF-OH}]_0$. The red lines indicate R_2^0 , where the R_2^0 rates for the free and bound states are 5 and $15\ \text{s}^{-1}$, respectively. The gray area indicates the concentration ratios that give R_{ex} rates from 3 to $25\ \text{s}^{-1}$. A similar plot for the pKID/KIX system⁶ is shown in Figure S5. (b) R_2 dispersion profiles at concentration ratios of 0.97, 0.98, 0.99, and 1. τ_{CP} indicates the delay between successive ^{15}N 180 pulses in the CPMG sequence.

the forward rate is the key factor that determines the amplitude of R_{ex} . At equimolar concentrations of HIF–OH and TAZ1, the forward rate is very fast compared to the chemical shift difference

between the free and bound states ($[\text{TAZ1}]k_{\text{on}} = 10883\ \text{s}^{-1}$; $\Delta\omega_{\text{FB}} = 1675\ \text{rad}\cdot\text{s}^{-1}$ (3.78 ppm) at ^{15}N frequency of 60.8 MHz). This is the reason why no R_2 dispersion was observed at 1:1 concentration ratio. Figure 2a suggests that it should be possible to observe R_2 dispersions that satisfy the criterion that R_{ex} be in the range ~ 3 to $25\ \text{s}^{-1}$ for concentration ratios from 0.97 to 1. However, simulations of the resulting dispersion profiles (Figure 2b) show that R_2^{eff} does not converge to R_2^0 with experimentally attainable ^{15}N 180° pulse repetition rates ($1/\tau_{\text{CP}}$) so that the derived kinetic and thermodynamic parameters will be unreliable. Therefore, we conclude that when the k_{on} is very fast, dispersion curves should be measured for the free state of a protein in the presence of substoichiometric amounts of the binding partner.

In summary, despite the absence of observable R_2 dispersions for the bound state of HIF–OH, we have obtained R_2 dispersion profiles of HIF–OH sufficient to derive kinetic and thermodynamic parameters by using substoichiometric concentrations of TAZ1. Although the relaxation rates of the free resonances were analyzed, the chemical shifts of the unobservable bound state could be determined by fitting the dispersion data. In the rather common case where bound peaks are unobservable because of intermediate exchange, relaxation dispersion measurements for free ligand resonances could provide chemical shifts and hence valuable structural information for the complex. By careful optimization of the concentration ratio, the R_2 dispersion method should be generally applicable for studying a wide range of protein–protein, protein–nucleic acid, and protein–small molecule interactions.

Acknowledgment. This work was supported by Grant CA 96865 from the National Institutes of Health and by the Skaggs Institute for Chemical Biology. J.C.L. was the recipient of an American Cancer Society postdoctoral fellowship. We thank Dr Maria Yamout for valuable discussions and for unpublished ITC data.

Supporting Information Available: Details of sample preparation, NMR titration of $[^{15}\text{N}]$ -HIF–OH with TAZ1, ^{15}N R_2 dispersion experiments, fitting of R_2 dispersion profiles, and simulation of R_2 dispersion profiles. This material is available free of charge via the Internet at <http://pubs.acs.org>.

References

- (1) Loria, J. P.; Rance, M.; Palmer, A. G. *J. Am. Chem. Soc.* **1999**, *121*, 2331–2332.
- (2) Mulder, F. A.; Mittermaier, A.; Hon, B.; Dahlquist, F. W.; Kay, L. E. *Nat. Struct. Biol.* **2001**, *8*, 932–935.
- (3) Boehr, D. D.; McElheny, D.; Dyson, H. J.; Wright, P. E. *Science* **2006**, *313*, 1638–1642.
- (4) McCammon, J. A.; Harvey, S. C. *Dynamics of Proteins and Nucleic Acids*; Cambridge University Press: Cambridge, 1987.
- (5) Korzhnev, D. M.; Salvatella, X.; Vendruscolo, M.; Di Nardo, A. A.; Davidson, A. R.; Dobson, C. M.; Kay, L. E. *Nature* **2004**, *430*, 586–590.
- (6) Sugase, K.; Dyson, H. J.; Wright, P. E. *Nature* **2007**, *447*, 1021–1025.
- (7) Dames, S. A.; Martinez-Yamout, M.; De Guzman, R. N.; Dyson, H. J.; Wright, P. E. *Proc. Natl. Acad. Sci. U.S.A.* **2002**, *99*, 5271–5276.
- (8) Freedman, S. J.; Sun, Z. Y.; Poy, F.; Kung, A. L.; Livingston, D. M.; Wagner, G.; Eck, M. J. *Proc. Natl. Acad. Sci. U.S.A.* **2002**, *99*, 5367–5372.
- (9) Lando, D.; Peet, D. J.; Whelan, D. A.; Gorman, J. J.; Whitelaw, M. L. *Science* **2002**, *295*, 858–861.
- (10) Berg, O. G.; von Hippel, P. H. *Annu. Rev. Biophys. Biophys. Chem.* **1985**, *14*, 131–160.
- (11) Eisenmesser, E. Z.; Bosco, D. A.; Akke, M.; Kern, D. *Science* **2002**, *295*, 1520–1523.
- (12) Tollinger, M.; Skrynnikov, N. R.; Mulder, F. A.; Forman-Kay, J. D.; Kay, L. E. *J. Am. Chem. Soc.* **2001**, *123*, 11341–11352.

JA0762238